

**GLOBAL APPLICABILITY OF ULTRAMAFIC SERPENTINITE AND
CARBONATION MAGNETIC MAPPING**

An Undergraduate Research Scholars Thesis

by

PAIDEN PRUETT

Submitted to the Undergraduate Research Scholars program at
Texas A&M University
in partial fulfillment of the requirements for the designation as an

UNDERGRADUATE RESEARCH SCHOLAR

Approved by Research Advisor:

Dr. Masako Tominaga
Dr. Michael Pope

May 2019

Major: Geophysics B.S.

TABLE OF CONTENTS

	Page
ABSTRACT.....	1
ACKNOWLEDGMENTS	2
NOMENCLATURE	3
CHAPTER	
I. INTRODUCTION	5
Background.....	5
Geology.....	6
Goals	7
II. METHODS	9
Field Work	9
Field Measurements	10
Forward Modeling	11
Magnetic Experiments	12
III. RESULTS	14
In-Situ Measurements	14
Magnetic Measurements	15
Magnetometer	18
IV. DISCUSSION	21
Dichotomy.....	21
Consistency	22
V. CONCLUSION.....	23
WORKS CITED	24

ABSTRACT

Global Applicability of Ultramafic Serpentinization and Carbonation Magnetic Mapping

Paiden Pruett
Department of Geology and Geophysics
Texas A&M University

Research Advisors: Dr. Masako Tominaga and Dr. Mike Pope
Department of Geology and Geophysics
Texas A&M University

Throughout the Earth's lithosphere, from its formation at spreading centers to its termination at subduction and/or obduction environments, serpentinization and carbonation processes of mantle rock are recognized as important contributors in the global carbon cycle on Earth. Understanding the extent of the serpentinization and carbonation process in-situ is, thus a critical first step in deciphering the carbon cycle. We aim to assess the global applicability of potential field measurements to monitor in-situ serpentinization-carbonation progression in mantle peridotite, based on the premise that magnetite abundances correlate with the progress of the carbonation reaction (Tominaga et al., 2017). We collected 5 representative samples along a transect of fully exposed upper mantle covering the full range of carbonation sequences on the Vancouver Ophiolite in Atlin, Canada. Based on field observations, we identify that the alteration stages along the transect sequentially range from harzburgite to serpentinized harzburgite, serpentinite, and listvenite. We conducted rock magnetic measurements on the samples, including Frequency-Dependent Susceptibility, First-Order Reversal Curve (FORC), Zero-Field Cooling (ZFC) and Temperature Dependent Susceptibility, to determine magnetic domain states, changes in domain state with variations in grain size, mixing of magnetic sources,

and the dominant magnetic mineral in the samples. Preliminary, first-order results from these magnetic experiments, in addition to Superconducting Quantum Interference Device (SQUID) microscopy, indicate that ferromagnetic minerals are dominant in the serpentinized samples, whereas paramagnetic minerals are dominant in the carbonated samples. Crustal gravity and magnetic anomaly measurements, analyzed with the rock sample measurements, manifest consistent results to previous studies of altered ultramafic rocks elsewhere, suggesting that the hypothesis of the global applicability of potential field methods as a monitoring scheme for serpentinization-carbonation reactions is viable.

ACKNOWLEDGEMENTS

The National Science Foundation (NSF) and the National Aeronautics and Space Administration (NASA) provided funding for the fieldwork associated with this project. The authors acknowledge and say thanks to the facilities, scientific aid, and technical assistance of the Massachusetts Institute of Technology EAPS Department, Curtin University, and the University of Minnesota's Institute for Rock Magnetism.

Noah Vento and Estefania Ortiz conducted fieldwork and made contributions during their time at Texas A&M. Mr. Vento and Ms. Ortiz were undergraduate and graduate students, respectively, in the Department of Geology and Geophysics that began the project and passed off the torch when graduating. A special thanks to John Greene, a Ph.D. student in the same department at Texas A&M, that assisted in project background, software assistance, and communication liaison when asked.

Curtin University's Dr. Andreas Beinlich provided the geochemical analysis and Massachusetts Institute of Technology's Dr. Eduardo Lima provided the SQUID Microscopic Imaging and 2G measurements. Dr. Patrick Fulton assisted in the fieldwork at the Atlin Site and helped process some of the field data for the project during his time as an assistant professor at Texas A&M University,

NOMENCLATURE

Mya	Million years ago
CCT	Cache Creek Terrane
GMT	Generic Mapping Tool
FORC	First Order Reversal Curve
ZFC	Zero Field Cooling
FDS	Frequency-Dependent Susceptibility
TDS	Temperature-Dependent Susceptibility
SQUID	Superconducting Quantum Interference Device

CHAPTER I

INTRODUCTION

Background

From the lithosphere's formation at spreading centers to its termination at subduction and/or obduction environments, serpentinization and carbonation processes of mantle rock have been recognized as part of the long-term carbon sink in the global carbon cycle on Earth. Understanding the extent of serpentinization and carbonation process in lithosphere is therefore crucial to estimate its influences to tectonics, deep biosphere, and ocean-atmospheric chemistry. Based on our understanding of the first order reaction equation of these processes, we identify that the processes correlate to the production and consumption of magnetically susceptible minerals, such as magnetites. We propose that the in-situ potential field measurements, which are sensitive to the amount of these minerals at each of the reaction stages, can be utilized as a monitoring scheme for tracking in situ serpentinization and carbonation processes. Towards this goal, we conducted field measurements that are ground-truthed by conventional rock magnetic experiments, SQUID microscopy, and demagnetization experiments. In order to best understand the crustal structure and field relations, we focus on an ophiolite section for our research experiment. Our survey site is located in Atlin, Northern British Columbia in Canada (Figure 1a) apart of the Atlin Ophiolite is monarch mountain where we observe 100% exposure of ultramafic crust (Figure 1b) that exhibits a full spectrum of serpentinization and carbonation processes, transitioning from serpentinized harzburgite to serpentinite and to carbonates.

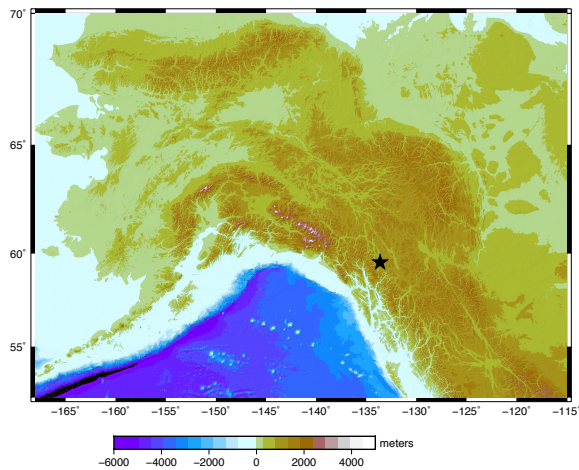


Figure 1a. Northwestern part of the North American Continent created in GMT. The star represents the location of the investigating site.

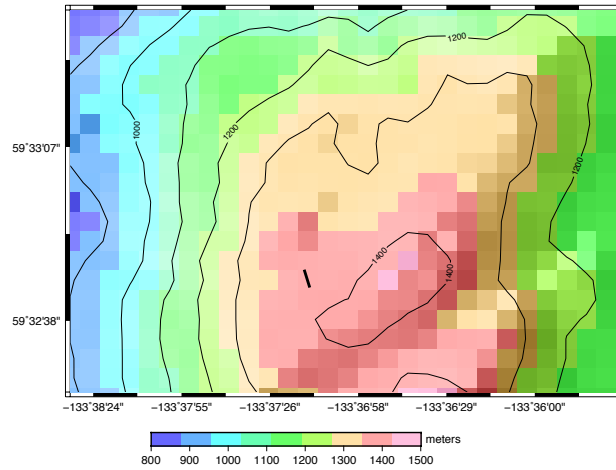


Figure 1b. Topographic map of Monarch Mountain in Atlin, British Columbia with a representative dash of the site location transect created in GMT.

Geology

The serpentinization and carbonation processes of mantle peridotite are intrinsically related to the production and consumption of magnetite that should be a mineral contributing to changes magnetic susceptibility and magnetization, detectable by potential field measurements. Understanding regarding the carbonation processes of ultramafic rocks has been mostly from petrological and geochemical contributions. With peridotite being one of the primary rock types composing the Earth's lithosphere, investigations of how signals respond to these processes could play a large role in determining, at a large scale, if these processes can be beneficial for in situ carbon dioxide sequestration in an ultramafic formation. The ultramafic cumulates range from weakly to moderately serpentinized harzburgite, serpentinite, and listvenite, in addition to transitional assemblages such as partially carbonated serpentine (Ash and Arksey, 1990).

The Atlin ultramafic complex represents an upper mantle section of the Tethyan oceanic lithosphere tectonically obducted during the Jurassic period. The Atlin ultramafic allochthon and accretionary complex obducted onto the Stikinia and Cache Creek Terranes during Jurassic amalgamation and accretion period (Ash and Arksey, 1990; Johnston and Borrel, 2006). The

Atlin complex originated from the Cache Creek Terrane (CCT) forming at spreading ridges above an oceanic hotspot on the eastern side of the South Chinese Crustal Blocks in the Paleotethys Ocean (Johnston and Borrel, 2006). While remaining in the northern hemisphere, an enclosement of the ocean basin by the CCT moving towards and accreting onto the North American craton occurred approximately 180 Mya with the Atlin ocean crust then obducting onto land approximately 140 Mya (Figure 2).

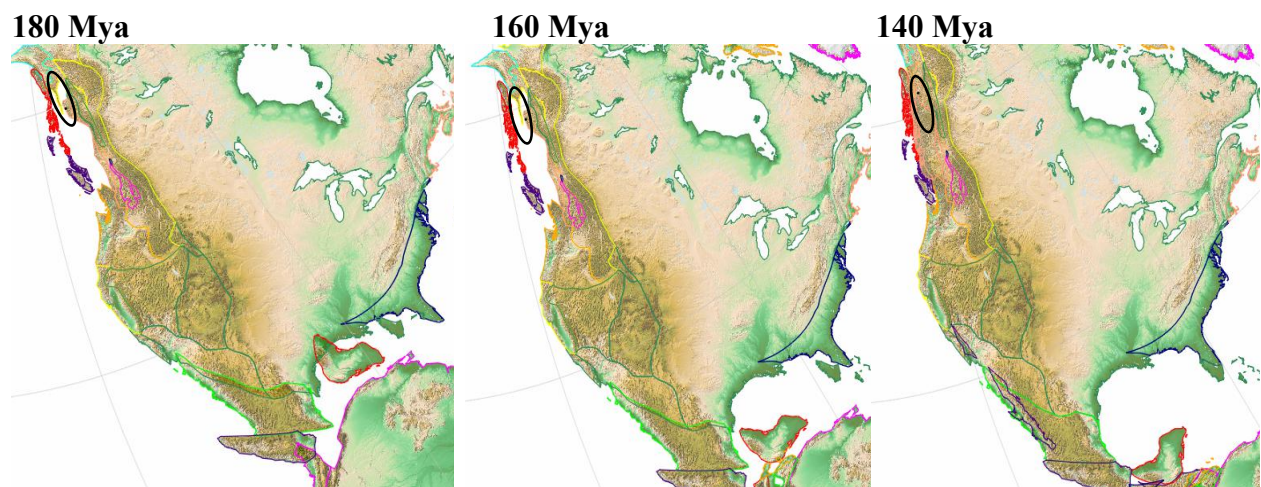


Figure 2. Paleo-topographic aerial maps of the North American Continent to its current configuration progressing from 180 Mya to 140 Mya in increments of 20 million years. Plate reconstruction produced with GPlates.

Goals

The objective of the study is to establish a globally applicable novel, field-based, high resolution surface geophysical monitoring scheme of in situ metasomatic processes to test the hypothesis that potential field values correlate with the degree of naturally occurring carbonation of mantle peridotite due to changes in the magnetite abundance throughout the reaction process. Two tribulations of the study include the variations of metasomatic reactions on tectonic setting and water chemistry and the limited information about magnetic carriers that allow for the signal to be measured. Field observations were conducted along with geochemical analysis and rock

magnetic experiments to resolve these issues. Through relating the rock magnetic experiments with the reactions occurring and correlating the experiments with the field measurements through forward modeling, we aim to establish the scheme of magnetic mapping in tracing the serpentinization-carbonation reactions.

CHAPTER II

METHODS

Field Work

The site location of Monarch Mountain in Atlin, British Columbia was visited in September of 2017 by a team of co-authors. In the field, 40 samples were collected and at sample sites, a line on the outcrop was marked, measured, and GPS coordinates and gravity and magnetic measurements were taken. The team collected rock magnetic susceptibility and gravity data along two transects. The first transect was 60 meters long and was composed of predominantly harzburgite and dunite -- highly ultramafic rocks (Figure 3). The second transect was 100 meters long and represented a full carbonation-serpentinization sequence from harzburgite to listwanite (Figure 3). The later, prioritized transect was 100 meters long and represented a full carbonation-serpentinization sequence from harzburgite to listwanite. Samples follow the naming format: Data collected - rock type - distance along transect (i.e. Gravity Magnetic – Listvenite Serpentinite Harzburgite - 39 meters along transect).

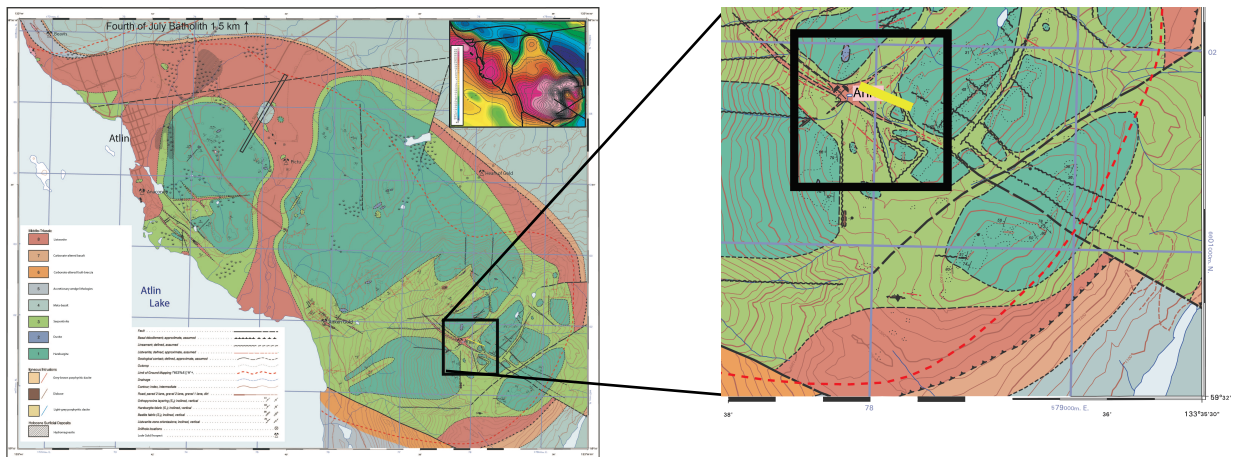


Figure 3. Lithological Boundary Map of Atlin site with marked survey transect (yellow line).

We collected 5 representative samples from each lithological unit that we observed along our survey transect (Figure 4). In order to understand the crustal scale relative changes in the magnetic anomaly amplitudes, we conducted potential field measurements using BGM gravity land meter and a APS 3 axis handheld magnetometer. Our survey transect is approximately 100 meters and measurements were taken at every half to seven meter sampling intervals. Our preliminary data reduction to both free air and bouguer gravity anomalies and total magnetic field measurements and models suggest that the field values show its maximum strengths over the serpentized harzburgite section and decreases along the transect towards carbonate sections. The magnetic and gravity field measurements collected were processed to account for multiple parameters.

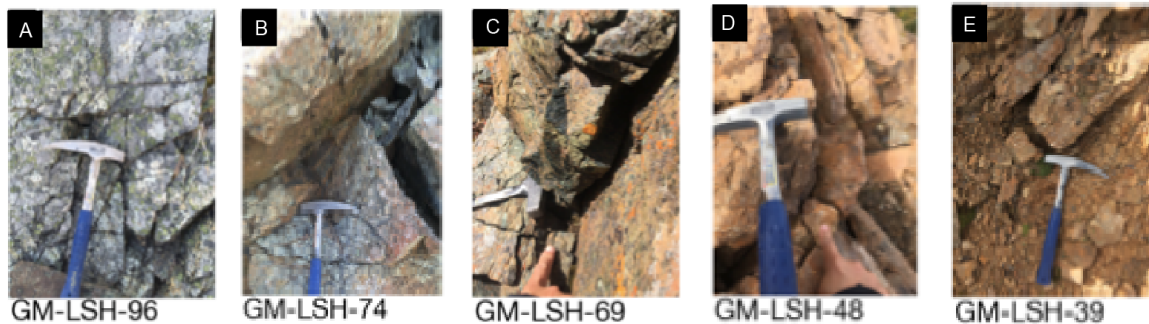


Figure 4. Sample picture taken at the research site showing the reaction progress.

Field Measurements

Magnetic data processing involved converting three coordinate values into standard units to calculate the total magnetic field and removing the Earth's main field using the International Geomagnetic Reference Field (IGRF) model (International Association of Geomagnetism and Aeronomy, 2010) value determined at the middle of the transect. Since the measurement was only taken over 100 m, relatively small to the IGRF scale, the center of the line, 50 m, was

chosen to represent the IGRF value for the entire surveying line. To average the total magnetic field for each location, each distance marker was associated with a range of measurements. The average for repeat location measurements was calculated. These averages for the distance markers were used to plot the anomaly against the distance along the transect. Gravity data processing entailed corrections using GravProcess: A MATLAB software to process campaign gravity data and evaluate the associated uncertainties. (Cattin et al., 2015) Tide, pressure, and instrumental drift corrections applied to the raw gravity data generate relative, observed gravity values. Removing the free air correction from the observed gravity values calculates the Free Air Gravity Anomaly. Following the calculation, the Canada digital elevation model (DEM) was utilized to perform the terrain correction on the gravity data. Removing the terrain attraction from the Free Air Gravity Anomaly gives the Bouguer Gravity Anomaly values. Both anomaly trends plotted along the survey transect distance to show gravitational strengths along the reaction path.

Forward Modeling

Conducting magnetic forward modeling enabled the region and rock magnetic properties to be constrained and determined by comparison of models' similarity to the in-situ magnetic measurements. Multiple forward models created utilizing the method in Talwani and Hertzler (1964) show the magnetic signals' strengths over the serpentinization-carbonation reaction. Regional geologic background with plate tectonic reconstruction using GPlates software (Matthews et al., 2016) constrained the inclination and declination parameters during the time of obduction. Combinations of changing input parameter values were trial tested to find values that best fit the trend of field measurements (Table 1).

Table 1. Forward Modeling Input Parameters.

Input	Value(s)	Input	Value(s)
Polarity	Positive, Normal	Layer Thickness	25 meters
Magnetization	0.1 through 4 A/m	Remanent Inclination	65°
Block Length	Transitional	Remanent Declination	47.68°
Sampling Interval	2 meters	Ambient Inclination	75.6493°
Profile Azimuth	161.71°	Ambient Declination	19.609°

Magnetic Experiments

A range of rock magnetic experiments and microscopic imaging were conducted on the samples, focusing on the 5 prioritized samples. At the Institute for Rock Magnetism (IRM) at the University of Minnesota, a group of student co-authors conducted a suite of state-of-the-art magnetic experiments on Atlin rock samples in order to fully characterize the population of mixing magnetic sources in the samples quantitatively. At the IRM, the team used a superconducting susceptometer (MPMS), vibrating-sample magnetometer (VSM), and Kappabridge high-temperature susceptometer (Kappa) to perform magnetic experiments on the Atlin samples. Samples from transect 2 (GM-LSH-39, 48, 69, 74, and 96) were prioritized over all other samples as these represented the full carbonation/serpentinization sequence from Atlin. The MPMS was used to measure direct current (DC) zero field cooling/field cooling (ZFC/FC) and alternating current (AC) frequency-dependent susceptibility (FDS). The VSM was used to measure hysteresis loops, backfield curves, and first-order reversal curves (FORC). The Kappa was used to measure temperature-dependent susceptibility (TDS). At Professor Benjamin Weiss' Paleomagnetic laboratory at the Department of Earth, Atmospheric, and Planetary

Sciences of the Massachusetts Institute of Technology, samples were put through a 2G Enterprises Superconducting Rock Magnetometer and 2G Superconducting Quantum Interference Device to measure demagnetization incremental steps and remanent magnetizations, respectively. Measurement results will be further discussed and shown in the results section.

CHAPTER III

RESULTS

In-Situ Measurements

Our preliminary data reduction to both free air and bouguer gravity anomalies and models suggest that the field values show its maximum strengths over the serpentinitized harzburgite section and decrease along the transect. (Figure 5). The total magnetic field measurements show an increase in magnetic anomaly along towards sample 39 to the 0 meter (m) mark of the transect. The blue points on the middle graph applies to the magnetization values used for the model (solid red line). Higher magnetization values unexpectedly correspond to the lower magnetic anomaly values.

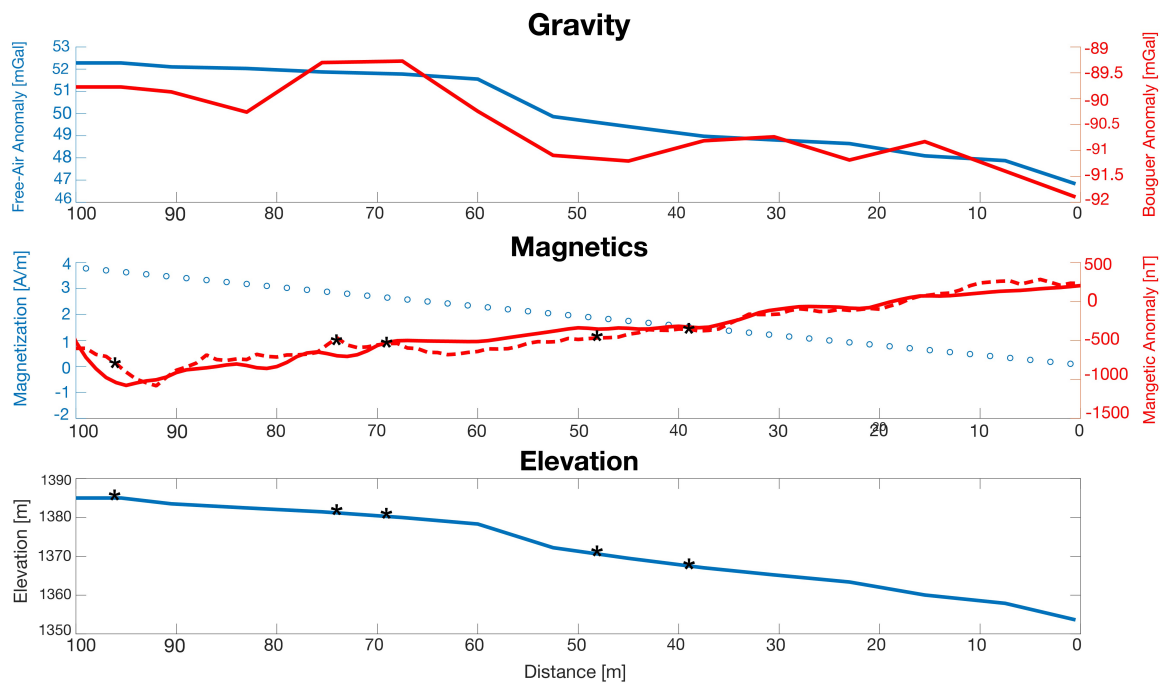


Figure 5. Processed Gravity, Magnetics, and Elevation measurements. Magnetic model presented by the dashed, red line. Black points represent the location of samples collected.

Magnetic Measurements

The Temperature Dependent Susceptibility (TDS) measurements (Figure 6) were conducted in order to determine the types of magnetic minerals by observing significantly different cooling patterns between serpentinized harzburgite and other samples. As samples are heated, reactions and changes in mineralogy are capable to occur. After the initial heating, the sample is cooled to either the same mineralogy as seen with the same cooling path or where mineralogical changes observed through different cooling paths are displayed. Similar cooling and heating paths are characteristic of ferromagnetic minerals, while paramagnetic minerals cooling paths do not follow their heating paths. Samples 96 and 74 show similar heating and cooling paths while samples 48 and 39 do not follow the same paths. Sample 69 shows a combination of the two patterns as the cooling path follows until the sharp susceptibility increase on temperature decline where it separates from the heating path. Based on their Curie temperatures, recognized as drops in susceptibility, magnetites are the dominant minerals in the harzburgite samples and other rock types likely show a more complex mixture of magnetic and non-magnetic minerals.

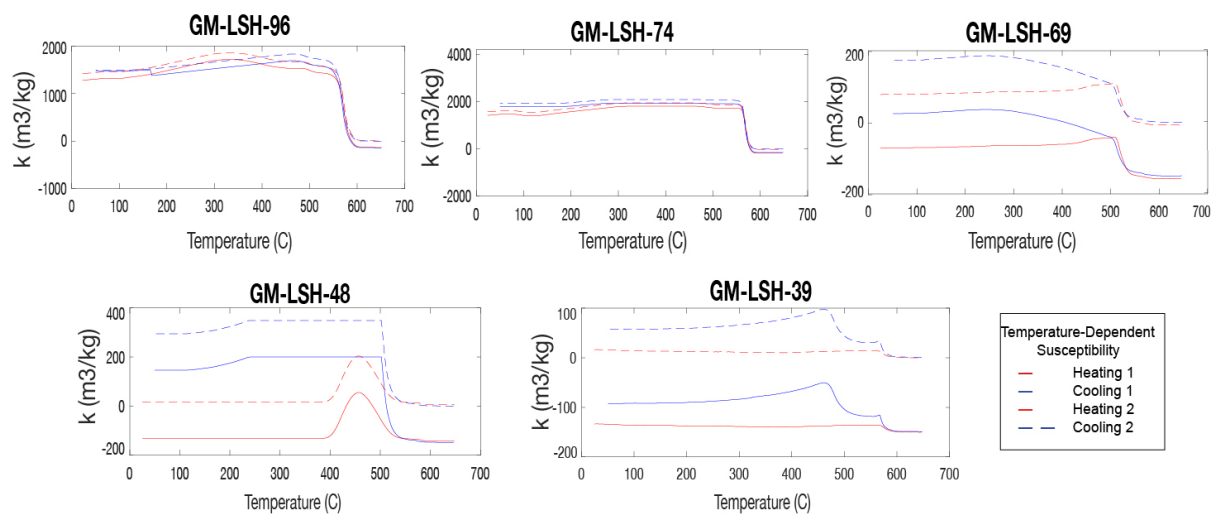


Figure 6. Temperature Dependent Susceptibility graphs show multiple heating and cooling paths.

To determine the coercivity characteristics of dominant mineral assemblages, Hysteresis (Figure 7) and Frequency Dependent Susceptibility (FDS) analyses (Figure 8) were completed. Hysteresis curves (Figure 7) show saturation magnetization and coercivity values. The curves transition from gradual to steep slopes, exhibiting a weakening resistance against the external field. A strong resistance to the externally applied field suggests that the sample contains a strong magnetic field of its own, as seen at the beginning of the transect in sample 96. As the resistance of a sample quickly folds and adopts the external field, the originating field strength is predicted to be small or weak as seen towards the end of the transect in sample 39. In the carbonate section, saturation is not reached suggesting possible diamagnetic minerals opposing the magnetic field.

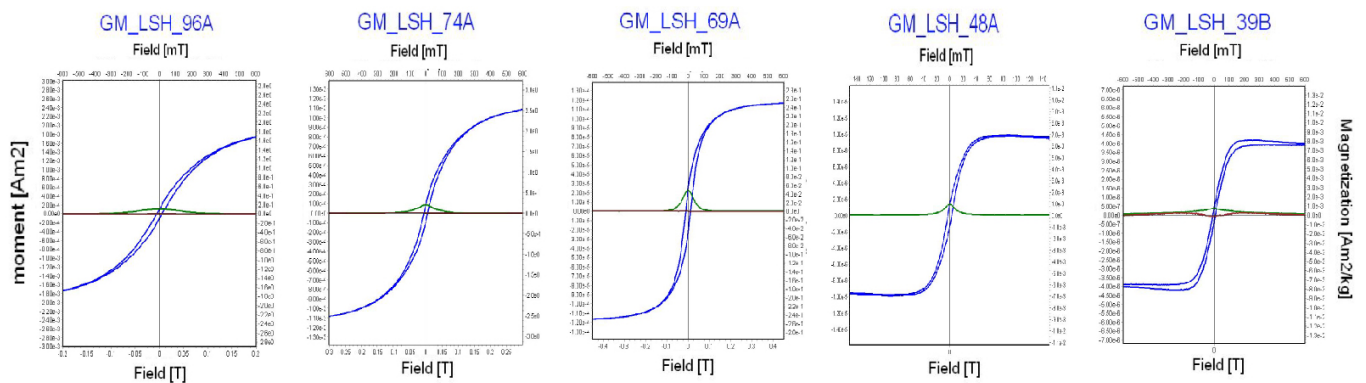


Figure 7. Hysteresis plots showing resistibility to an externally applied magnetic field.

Frequency Dependent Susceptibility curves (Figure 8) exploits the grain relaxation times by enabling the comparison of magnetization at different frequencies. Grains with frequencies slower than the reaction time allow more time for grains to absorb remanent magnetization and increase susceptibility. FDS measurements are conducted with an alternating current that records magnetic susceptibility with a changing magnetic field. For ferromagnetic material, the susceptibility increases as temperatures increase above room temperature (100 K). While for

paramagnetic material, susceptibility is proportional to magnetic minerals. At room temperature, if the amount of magnetic minerals is low then the susceptibility will be lower than previously, before reaching room temperature. These, respectively, are seen in samples 96 and 39 with sample 69 exhibiting a transitional stage between the two end-members of the prioritized transect. Also, these measurements show a presence of superparamagnetic grain size minerals, likely pepper flake type magnetites that are commonly observed in serpentinized rocks whereas measurements on carbonate samples do not show any signs of the presence of these minerals.

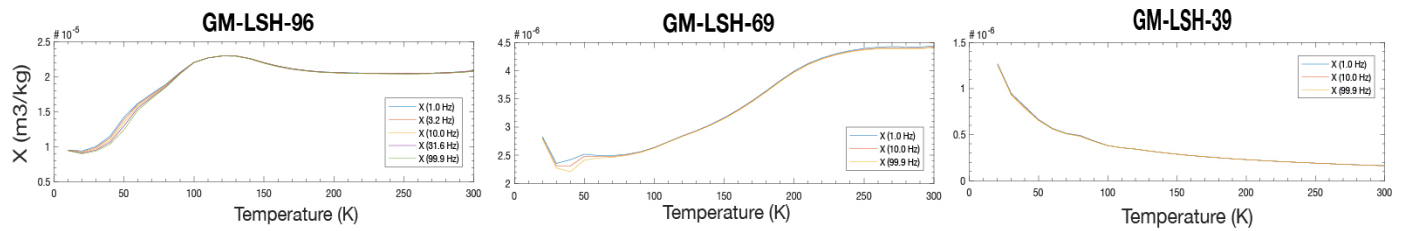


Figure 8. FDS graphs portraying grain domain characteristics.

We used First Order Reversal Curves analysis at the IRM in order to determine the grain size distribution of magnetic minerals in the samples. With their sensitivity to mineral grain sizes, FORC diagrams (Figure 9) show the coercivity characteristics of dominant mineral assemblages, exhibiting similar dichotomy between the serpentinized samples and the carbonate as already seen. When looking at the domain size assemblages in the FORC measurements, the 96, 74, and 69 samples show near zero interaction distribution along the vertical axis and a range of coercive distributions along the horizontal. The 48 and 39 samples show more interactions distributed along the vertical, H_u (T) axis and low coercivity nearing zero along the horizontal axis. These distributions are characteristic of single and multi-domain states, respectively.

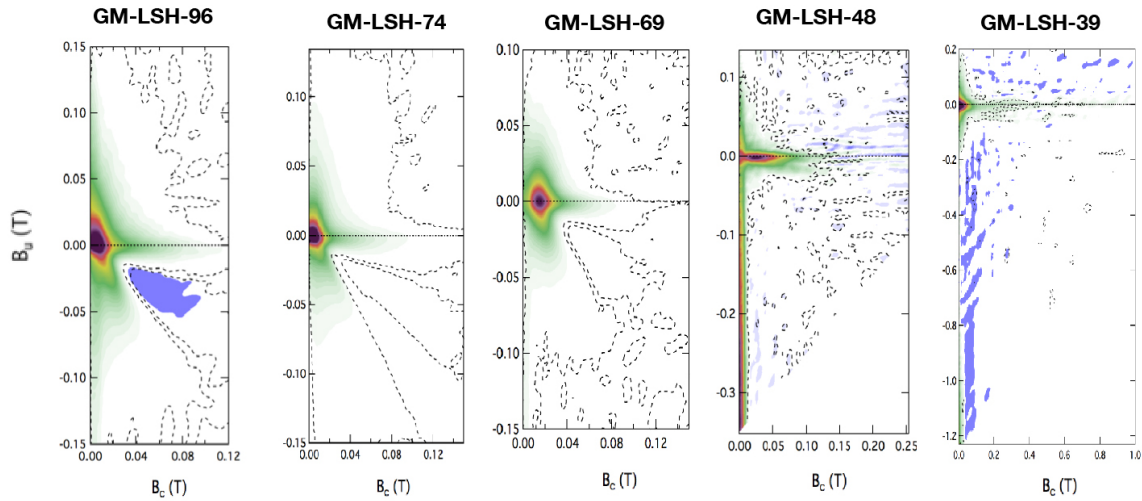


Figure 9. FORC measurements displaying coercive and interaction distributions.

Magnetometer

The 2G Superconducting Quantum Interference Device produced images (Figure 10) of the total magnetic field of the sample mounted by imparting anhysteretic remanent magnetizations (ARM) with a bias field of 100 nanoteslas (μT) and a peak alternating field of 260 microteslas (mT) to activate magnetic sources. The top panels show the natural remanent magnetic field with the bottom panel showing the ARM. Each view shows analogous total magnetic field data to that of what we measured in the field with our handheld magnetometers at a finer scale. An increase in total magnetic field strength occurs when comparing sample 96 and 74 but decreases in sample 69 seen in both the NRM and ARM images. Samples 48 and 39 show a nearly non-existent total magnetic field strength, in NRM and ARM images. Overall, we observe the distinctive dichotomy that has divided the samples into two groups with more detailed information.

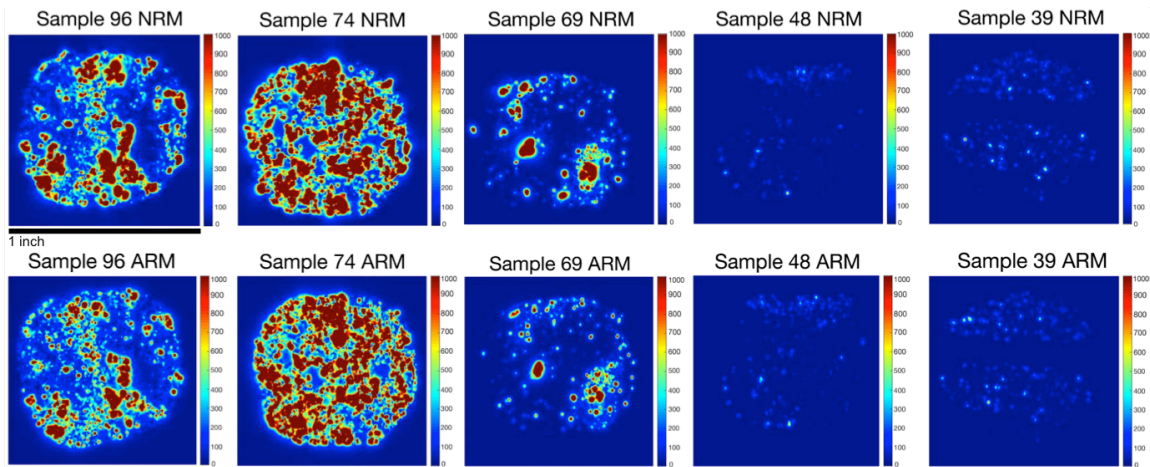


Figure 10. SQUID measurements of the NRM and ARM of each individual sample.

The 2G Enterprises Superconducting Rock Magnetometer demagnetized each sample with an alternating field to see separate magnetization components. A maximum alternating field of 1450 Gaussian with intervals of 10 was applied to the total sample thin section producing trends that show similarity to some multi component magnetization stages that have been observed in oceanic serpentinized gabbro sample. Samples 96, 74, and 69 portray a more unified directional demagnetization, as visually guided with the black arrows. A less directionally unified, more dispersed demagnetization steps. The measurements (Figure 11) are plotted in an north-south, geographic, orthographic projection with the red, inclination points projected on the horizontal plane and blue, declination points projected on the vertical plane.

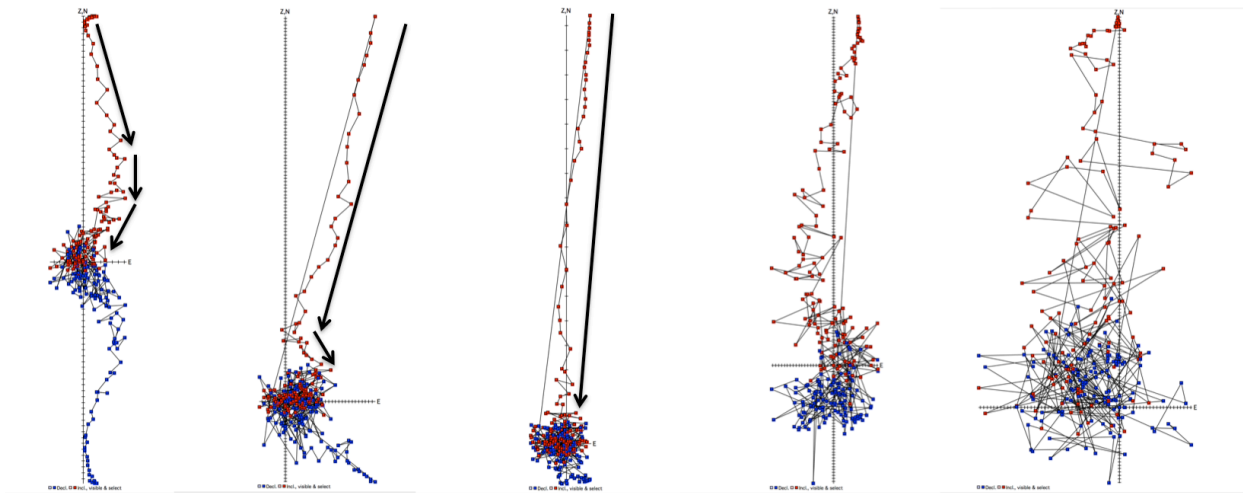


Figure 11. 2G data displaying an interval demagnetization process.

CHAPTER IV

DISCUSSION

Overall, our magnetic measurements exhibit consistent magnetic characters at multiscales from the outcrop measurements microscopic scales. The most striking observation is that SQUID measurements show a strong, total magnetic field in the samples: 96, 74, and 69, with a nearly absent total field in the 48 and 39 samples. These images portray the transition seen in the field, reiterated through the sample images. The preliminary petrological observations at the outcrop display consistent results with that of the Norway study (Tominaga et al., 2017). The petrological field observations exhibited transitional phases between the serpentinized and carbonated end-members along the transect. Tominaga et al. (2017) involved similar rock types in the sense of different carbonation phases along an ultramafic complex in an upper allochthon as well. Our survey transect, captures serpentinization stages of this metasomatic process, which was mostly lacking from the Norway field site and Tominaga et al. (2017)'s results thereof, allowing the stages regarding the whole reaction progress. We argue that our Atlin results are a manifestation of the magnetic signals from different scales through certain stages as being a monitoring scheme to track the serpentinization and carbonation processes in mantle peridotite.

Dichotomy

In detail, the rock magnetic results show almost a complete dichotomy of the magnetic characters in two separate groups: samples 96, 74 and 69 (hereafter group A) and then the samples 48 and 39 (hereafter group B). The SQUID measurements show different magnetic field strengths when comparing the samples in each group against each other. Magnetically, the FORC, hysteresis, and diagrams are principally identical between the samples of each group. Of

the FORC diagrams, the serpentinized samples display higher coercivity distributions while the 48 and 39 samples display higher interactive distributions and being nearly identical. Likewise, the shallow slopes in the 96 and 74 samples transition through 69 and rapidly steepen in samples 48 and 39 of the hysteresis measurements. These results highlight More apparent of a dichotomy is visualized in the 2G data with consolidated compared to dispersed demagnetization directions.

Consistency

The Frequency Dependent Susceptibility (Figure 8) plots indicate thoroughly different grain domain characteristics between the end-member transect samples. The increase and decreases in susceptibility of Samples 96 and 39 show the drastic change from ferromagnetic to paramagnetic minerals as ferromagnetic minerals hold the magnetization from the previous field until a maximum of susceptibility is reached while paramagnetic minerals do not. Sample 69 appears to show a transitional state between the 96 and 39 samples in the FDS plots. As equal heating and cooling paths portray the minerals' ferromagnetism's characteristic of permanent magnetization, the Temperature Dependent Susceptibility plots are consistent with the FDS plots. Seeing multiple samples associated with each processes proves beneficial as the previous Norway study had a greater emphasis on the rock carbonation.

CHAPTER IV

CONCLUSION

The samples 96, 74, and 69 correspond to the serpentinization phases of the overall reaction progression and possibly the first carbonation phase. Although our sample 69 appears to be the transitional sample, the placement of other samples, ex: 48, on the reaction path are unknown based on the results of the Norway study. This indicates that we indeed can utilize the magnetic data as a monitoring scheme, as hypothesized, but to the extent that we can capture the serpentinization to the first carbonate phase versus the complete carbonated phase. Conclusively, these signals can be employed to monitor in situ reactions and effect but not the gradual change occurring. These are the most comprehensive conclusions that can be drawn until the geochemical and petrological reports to ground truth what the magnetic measurements are suggesting are completed and received. Fully integrating remote sensing with laboratory rock magnetic experiments, geochemical, and petrological analysis allows for globally establishing the monitoring scheme to track the in-situ reaction progress.

Ongoing investigations are underway to explain the observational values in the magnetics data varying from the hypothesized. The field measurements resulted in higher magnetic anomalies above the hypothesized carbonated samples than the serpentinized samples. As viewed in the magnetics measurements, the samples have greater magnetic susceptibility, properties, and characteristics that contradict the magnetic anomalies for those same samples. The optimal combinations with the modeling parameters agree with serpentinization having higher magnetization values with rocks magnetizing during a time of normal polarity.

REFERENCES

- Ash, C.H., Arksey, R.L. (1990a) The listwanite-lode gold association in British Columbia. Geological Fieldwork 1989, A summary of Field Activities and Current Research, Province of British Columbia, Mineral Resources Division Geological Survey Branch, pp. 359–364
- Cattin, R., Mazzotti, S., Baratin, L. (2015). GravProcess: An easy-to-use MATLAB software to process campaign gravity data and evaluate the associated uncertainties. *Computers & Geosciences*, Vol. 81, pg. 20-7, <https://doi.org/10.1016/j.cageo.2015.04.005>.
- International Association of Geomagnetism and Aeronomy (2010): International Geomagnetic Reference Field - 11th Generation. National Geophysical Data Center, NOAA. doi:10.7289/V58050JN [May 2018]
- Johnston, S.T., & Borel, G.D. The Odyssey of the Cache Creek terrane, Canadian Cordillera: implications for accretionary orogens, tectonic setting of Panthalassa, the Pacific superwell, and break-up of Pangea. *Earth and Planetary Science Letters*, Volume 253, (2007), pp. 415-428.
- Matthews, K. J., Maloney, K. T., Zahirovic, S., Williams, S. E., Seton, M., and Müller, R. D., 2016, Global plate boundary evolution and kinematics since the late Paleozoic: Global and Planetary Change, DOI: 10.1016/j.gloplacha.2016.10.002.
- Tominaga, M., A. Beinlich, E. A. Lima, M. A. Tivey, B. A. Hampton, B. Weiss, and Y. Harigane (2017), Multi-scale magnetic mapping of serpentinite carbonation, *Nature Communications*, 8(1), doi:10.1038/s41467-017-01610-4